Supporting Information

Bulk heterojunction-induced ion transport in nanochannels array for light-enhanced osmotic energy conversion

Youfeng He, Liangqian Zhang, Liang Guo, Yutong Geng, Yan Ren, You Liu, Xia Fan,* Weimin Liu,* Jin Zhai,* Pengfei Wang and Lei Jiang

Youfeng He, Liangqian Zhang, Yutong Geng, Yan Ren, You Liu, Xia Fan,* Jin Zhai,* and Lei Jiang

School of Chemistry, Beihang University, Beijing 100191, P. R. China

Liang Guo, Weimin Liu,* and Pengfei Wang

Technical Institute of Physics and Chemistry, Chinese Academy of Sciences, Beijing 100190, P. R. China

E-mail: fanxia@buaa.edu.cn; zhaijin@buaa.edu.cn; wmliu@mail.ipc.ac.cn

Synthesis process of PT2

Materials: $FeCl_3$, 4-Bromobenzyl bromide, N,N-dimethyldodecylamine, thiophene-3-boronic acid, tetrakis (triphenylphosphine) palladium (0), 3-thiophene-acetic acid, methoxy-PEG-OH (MW. 2000) were purchased form J&K Chemical Co. and Alfa Aesar. Other reagents were purchased from Beijing Chemical Regent Co. All chemicals and materials used were used without further purification. $CHCl_3$ was distilled from CaH_2 under nitrogen.

Method: Poly (3-thiophene-phenyl-tridecyl ammonium bromide) (PT2) was synthesized according to our previous reported work.[1-3] In brief, compound 1 (N-(4-bromobenzyl)-N,N-dimethyldodecan-1-aminium bromide) was prepared by nucleophilic addition with 4-bromobenzyl bromide and N,N-dimethyldodecylamine in N_2 atmosphere and a mixed solvent (CH_2Cl_2 and CH_3OH). Compound 2 was obtained by SUZUKI reaction with compound 1 and thiophene-3-boronic acid with $Pd(PPh_3)_4$ as catalyst. Subsequently, PT2 was attained via oxidative polymerization taking PT2 as monomer catalyzed by $FeCl_3$ in anhydrous $CHCl_3$.
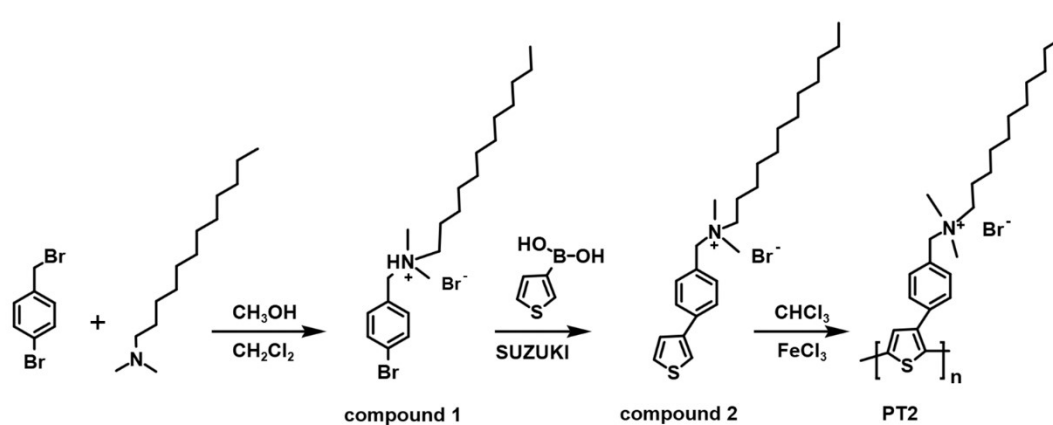

Figure A. Synthesis process of PT2.

The experimental steps of asymmetric modified Al$_2$O$_3$ nanochannels.

PT2(B)/N3(T) nanochannels: First, the prepared Al$_2$O$_3$ film was soaked in 30 wt% hydrogen peroxide and boiled for 1 h to activate the hydroxyl groups on the surface of the nanochannels. Next, after 6-hours chemical reaction in a constant temperature metal bath, the PT2 molecules were successfully grafted to the B segment of the nanochannel driven by the gravity and capillary force of the solution. The obtained Al$_2$O$_3$ film was then placed in a self-made cell, one of which was filled with N3 solution (2 mM) and the other was filled with ethanol solution. N3 molecules diffused from the high-concentrated side to the low-concentrated side, and then successfully modified to the T segment of the funnel-shaped channel after 2-hours electrostatic interaction. And the PT2(B)/N3(T) nanochannels were prepared successfully.

N3(B)/ PT2(T) nanochannels: First, the prepared Al$_2$O$_3$ film was placed in a self-made battery, one of which was filled with N3 solution (2 mM) and the other was filled with ethanol solution. N3 molecules diffused from the high- concentrated side to the low-concentrated side, and then modified to the B-segment of the funnel-shaped channel after 4 hours. PT2 molecules were then modified in a thermostatic metal bath. After 6 hours, the PT2 molecule was successfully grafted to the T segment of the nanochannel. And the N3(B)/PT2(T) nanochannels were successfully fabricated.

The irradiation position, wavelength, and intensity of the simulated light.

In this work, we synchronously applied light stimulation on both sides of the quartz window of the electrolytic cell. The light beam passes through the electrolyte and hits the surface and inner wall of the nanochannels. In the experiment, the light source is composite white light. The intensity range of light source is 100 W/m².
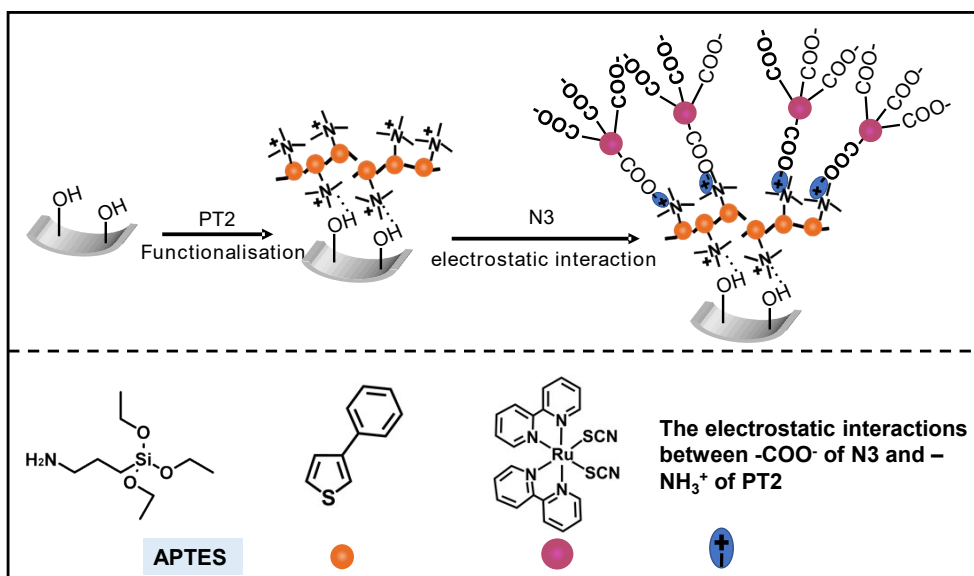
Figure S1. Schematic illustration of the experimental steps for constructing bulk heterojunction in the funnel-shaped Al_2O_3 nanochannels.

Modification of N3 in PT2-functionalized channel: The inner wall of the prepared Al_2O_3 nanochannel contains abundant hydroxyl groups, which interact with the functional groups of PT2 molecules to form hydrogen bonds, and the PT2-functionalized nanochannels were successfully prepared. Then, the carboxyl group of negatively charged N3 interacts with the amino group of PT2 through electrostatic interaction, so that N3 is successfully modified to the inner wall of the channel. After chemical modification, the B segment and T segment of the alumina nanochannel show positive and negative charges respectively.
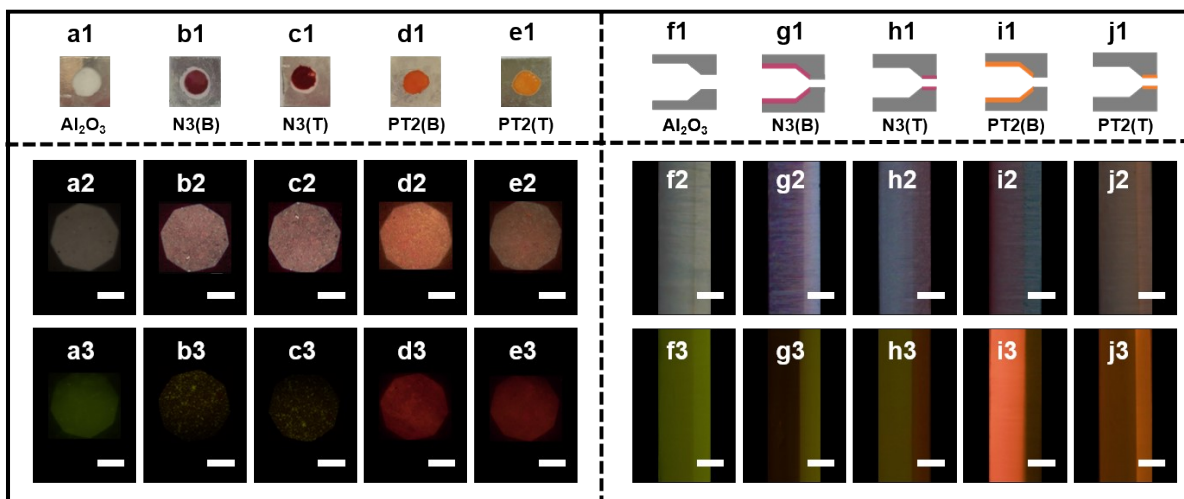
Figure S2. (a1-e1) Optical photographs of the upper surface of membranes (the upper surfaces refer to the top surface of B segment). (a2-e2) The optical and (a3-e3) the fluorescence microscope images of the upper surface of membranes. Scale bars: 100 μm. (f1-j1) Schematic diagrams of cross-section of asymmetric funnel-shaped channels. (f2-j2) The optical and (f3-j3) the fluorescence microscope images of the cross-sectional viewing. Scale bars: 20 μm.

As illustrated in Figure S3a1, the naked Al_2O_3 nanochannels membrane shows translucent state with a circle (0.25 cm^2) in optical diagrams. After modification, the color of membrane changes from the translucent to the color of the corresponding photo responsive molecules (N3 is purple and PT2 is orange) (Figure S3a1-3e1). A series of optical microscopy images (Figure S3a2-3e2) reveal that N3 and PT2 have been successfully modified onto the channels. Due to the different scattering and absorption effects between N3 and PT2, the fluorescence microscope images (Figure S3a3-3e3) also verify the successful modification of photo responsive molecules to a certain extent. In addition, the optical (Figure S3f2-3j2) and the fluorescence microscope images (Figure S3f3-3j3) of the cross-sectional viewing reflects that the state of channel is affected by modified molecules. Compared with the bare Al_2O_3 nanochannels, the clear color contrast can visually illustrate the successful grafting of N3 and PT2 molecules on the inner wall of funnel-shaped channels.
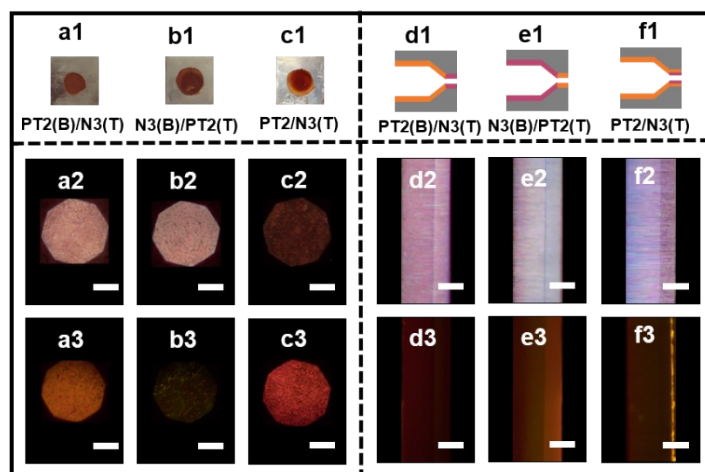
Figure S3. (a,b) A tip junction is formed by asymmetrically modifying N3 and PT2 molecules onto the two different segments of nanochannel. (c) A specific bulk heterojunction is established by modifying bilayers photo responsive molecules in specific segment of nanochannel. (a1-c1) Optical photographs of the upper surface of membranes. (a2-c2) The optical and (a3-c3) the fluorescence microscope images of the upper surface of membranes. (d1-f1) Schematic diagrams of cross-section of asymmetric funnel-shaped channel. (d2-f2) The optical and (d3-f3) the fluorescence microscope images of the cross-sectional viewing. Scale bars: 20 μm.
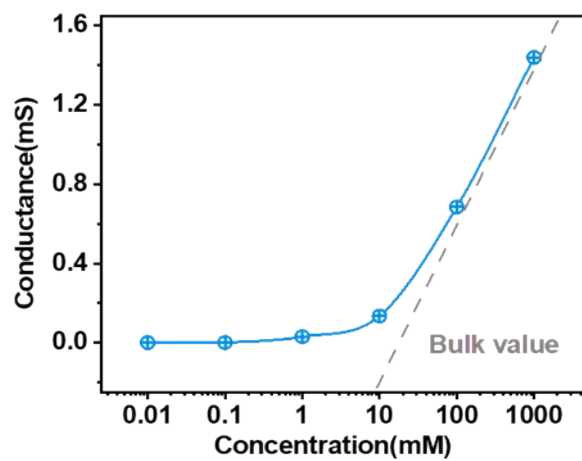
Figure S4. Conductivity versus KCl concentration for PT2/N3(T) nanochannels membrane.
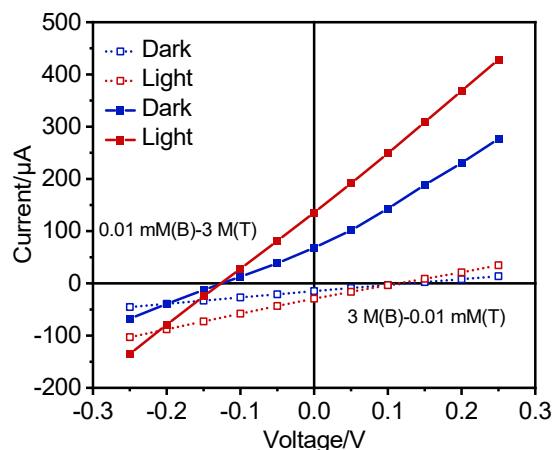
Figure S5. Two opposite configurations of concentration gradient were arranged to determine the superior direction of output performance. When the 3 M KCl solution facing the T-segment side and 0.01 mM KCl solution facing the B-segment side, the absolute values of I_{sc} and V_{oc} are 68.3 μA and 125.3 mV, respectively. When the 3 M KCl solution facing the B-segment side and the 0.01 mM KCl solution facing the T-segment side, the corresponding I_{sc} and V_{oc} change to 14.89 μA and 130.1 mV, which means that the calculated internal resistance increases. Hence, the preferential direction of ion transport across the PT2/N3(T) membrane is from N3 to PT2.
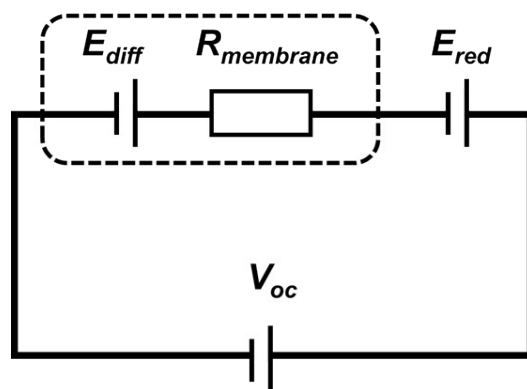
Figure S6. Equivalent circuit diagram of integrated nanofluidic energy converter. Generally, the measured V_{oc} is composed of the diffusion potential (E_{diff}) and the redox potential (E_{redox}) that occurs at electrode and solution interface. The E_{redox} can be obtained by replacing the selective PT2/N3(T) membrane with a non-selective silicon film containing a single pore with 100 μm-length window. In this case, the measured potential is only contributed by the redox reaction at the electrode and interface.

Supporting Note 1. Osmotic power harvesting

	V_{oc}	I_{sc}	P_{out}	E_{diff}	I_{diff}	P_{diff}
10 mM-0.5 M	118 mV	35 μA	34.3 W/m²	75 mV	20 μA	12.5 W/m²

The cation-selective PT2/N3(T) membrane was embedded in the two chambers of the self-made electrolytic cell, in which high-concentrated solution (0.5 M NaCl) was injected into the chamber towards the T-segment and the other chamber was filled with 10 mM NaCl. Ag/AgCl electrodes were used to collect currents under 50-fold salinity gradient. In this case, the system offered a theoretical output power density 34.4 W/m² according to Equation 1:

$$Pout = \frac{IscVoc}{4S} \qquad (S1)$$

where V_{oc} and I_{sc} are the reading open-circuit voltage value and short-circuit current value, respectively, and S is effective test area. [4] However, the net diffusion power density generated by ion diffusion merely was calculated to be 12.5 W/m² according to Equation 2 :

$$P_{diff} = \frac{E_{diff}^{2}}{4SR_{mem}} \qquad (S2)$$

where R_{mem} refers to the membrane resistance, E_{diff} is osmotic potential. After deducting the contribution of the reaction at the electrode to the V_{oc}, the resulting E_{diff} and I_{diff} are generated by ions diffusion under specific concentration gradient.

Reference

1   L. Guo, J.H. Ge, W.M. Liu, G.L. Niu, Q.Y. Jia, H. Wang and P.F. Wang, Tunable multicolor carbon dots prepared from well-defined polythiophene derivatives and their emission mechanism, *Nanoscale*, 2016, **8**, 729.

2   J.H. Ge, M.H. Lan, B.J. Zhou, W.M. Liu, L. Guo, H. Wang, Q.Y. Jia, G.L. Niu, X. Huang, H.Y. Zhou, X.M. Meng, P.F. Wang, C.S. Lee, W.J. Zhang and X.D. Han, A graphene quantum dot photodynamic therapy agent with high singlet oxygen generation, *Nat. Commun.*, 2014, **5**, 4596.

3   M.H. Lan, J.S. Wu, W.M. Liu, W.J. Zhang, J.C. Ge, H.Y. Zhang, J.Y. Sun, W.W. Zhao and P.F. Wang, Copolythiophene-Derived Colorimetric and Fluorometric Sensor for Visually Supersensitive Determination of Lipopolysaccharide, *J. Am. Chem. Soc.*, 2012, **134**, 6685-6694.

4   D.K. Kim, C.H. Duan and Y.F. Chen and A. Majumdar, Power generation from concentration gradient by reverse electrodialysis in ion-selective nanochannels, *Microfluid. and Nanofluid.*, 2010, **9**, 1215-1224.